Inversion-based 3D deblending of towed-streamer simultaneous source data using sparse TauP and wavelet transforms

Can Peng and Jie Meng, CGG*

Summary

We propose a 3D deblending method for towed-streamer simultaneous source data based on an L1 inversion algorithm. The approach pursues a sparse representation of 3D coherent signals that matches the blended data in a domain combining 2D TauP and 2D directional wavelet transforms. In this method a sparse 2D TauP transform is first applied in the common shot gather to focus coherent signals along channels to P traces. Subsequently, an L1 inversion algorithm based on the 2D high angular resolution complex wavelet transform (HARCWT) is used to deblend the signals of different sources for each common P gather. Since the shot domain TauP transform has good separation of the events according to their slopes, and the coherent signals across shots have sparse representation in the HARCWT domain, the method can achieve high-quality deblending results. The method was tested on a numerically blended field data set, and the result was an improvement over 2D HARCWT deblending channel by channel and even deblending with 3D HARCWT.

Introduction

In simultaneous source acquisition, multiple sources are allowed to shoot in a shorter interval than the conventional listening time. This increased shooting density results in considerable savings in time and cost of seismic surveys. It is no wonder that these acquisitions are attracting more and more industry attention (Beasley et al., 2012). The results of simultaneous source acquisition are data containing a blend of energy from multiple sources. The energy from each source in these blended data must be separated in a process known as deblending before conventional processing algorithms can be used.

Some deblending methods are based on coherence enhancement (Doulgeris et al., 2010; Beasley et al., 2011; Peng et al., 2013; Maraschini et al., 2012) which typically separate energy from the blended data iteratively. Other methods are based on sparse inversion algorithms to solve underdetermined linear systems that match the blended measurements with coherent signals of different sources that have sparse representations in a certain transform domain (Abma et al., 2010; Ayeni et al., 2011; Li et al., 2013). The iteration steps in sparse inversion algorithms are usually optimized in both the gradient direction and step size, and hence, with properly set parameters like constraint weights and the iteration number, good deblending results may be obtained without much human intervention.

Finding an optimal basis dictionary (i.e., a linear transform) to represent signals is important in sparse inversion-based methods. The coherent signals from a source in its own time frame should have a sparse representation in the basis dictionary. This means only a small number of bases should be required to reconstruct the coherent signals with high fidelity. On the other hand, the incoherent cross-talk energy from other sources can only be reconstructed by a large number of bases with small amplitudes. Other considerations of choosing the linear transform include computational cost, the size of the basis dictionary, and the type of blended data. Different transforms are used for deblending, such as TauP (Akerberg et al., 2008), curvelet (Kumar et al., 2015), 3D FK (Abma et al., 2010), among others. For blended OBN/OBC data, TauP transforms may be a good choice because the seismic events in common node gathers have well defined bounds in the slope ($1/c$, c is the water velocity), and they can be sparsely represented in a spatial window by the linear bases of TauP transforms. However, for towed-streamer data the randomness of the other source appears in common channel gathers, in which the slopes of events are bounded by large slowness ($2/c$) and events are less linear, especially in regions with strong diffractions or faults. Therefore, TauP transforms incur high computational cost for this type of data. 3D FFT is a relatively economical alternative, but the transformed data are less sparse in this domain than in the sparse TauP, curvelet, or HARCWT domain (Peng et al., 2013), leading to a large number of iterations in the inversion for high quality deblending. Curvelet transforms and HARCWT both allow sparse representations for coherent events in common channel gathers of towed-streamer data, and they are suitable for 2D deblending that is performed on common channel gathers one by one; however, when applied in 3D (deblending consecutive common channel gathers together), curvelet and HARCWT transforms create a substantially larger model space than the input data space. This increases both the computational and memory cost.

Compared with deblending for each channel gather separately based on 2D transforms, 3D deblending for several consecutive channel gathers together may lead to better results because it regards the coherence in both channel and shot directions and can recover some events that are not sufficiently coherent for sparse representation in the common channel domain but are coherent across channels (Maraschini et al., 2012). In this work we combine 2D sparse TauP and 2D HARCWT transforms to achieve 3D deblending for multiple channels without increasing much of the computational cost.

3D deblending using sparse TauP and wavelet transform

Method

In towed-streamer simultaneous source data, the seismic signals of all sources are coherent in common shot gathers, and the slopes of the seismic events are well bounded by the reciprocal of the water velocity. In the case when arrivals from different sources have conflicting dips, application of a 2D sparse TauP transform for each shot may partially separate these events according to their slopes. In the common channel domain, seismic events for the aligned source will be coherent and the cross-talk energy from other sources appears random. In this direction the coherent signals may have a sparse representation in the 2D HARCWT domain. Therefore, we propose the following workflow:

1. Apply a sparse 2D TauP transform to each common shot gather of a cable.
2. Sort to common P/shotpoint order.
3. Apply L1 inversion based deblending with 2D HARCWT for each common P gather.
4. Reorganize the deblended P traces to form the TauP models for all shots of all sources.
5. Perform reverse TauP transform for all shots of all sources.

The sparse TauP algorithm used here is similar to that described by Trad et al. (2003), which is based on iteratively re-weighted least-squares inversion. In the TauP transform, the P range is chosen from $-1/c$ to $1/c$, and the P interval can be determined by $1/N\Delta x f_m$, where N is the number of channels included in the TauP transform, Δx is the channel interval, and f_m is the highest frequency of the signal. Therefore the number of Ps can be estimated by $2N\Delta x f_m/c$. With commonly used channel intervals, e.g., 12.5 m, the number of Ps is smaller than $2N$, when $f_m < 120$ Hz. If the signal energy is concentrated in a small number of Ps, the iteration of step 2 is only required for those Ps. If this time saving exceeds the overhead cost of the sparse TauP and reverse TauP outside the iteration, the computational cost of this method may be even lower than that of 2D deblending based on HARCWT in common channels. Figure 1 shows the sparse TauP transform of some blended shot gathers and several common P gathers. The gathers were numerically blended with field data from two sources. Fewer seismic events and less cross-talk energy exist in a single common P gather than in a common channel gather due to the separation of events achieved by the sparse TauP transform. HARCWT is a directional, high-dimensional wavelet transform. It can separate coherent events based on their dip direction and local phase. For coherent events that can be sparsely represented by fewer bases, the corresponding coefficients are strong; on the other hand, random cross-talk energy results in smeared and weak coefficients in the transform domain.

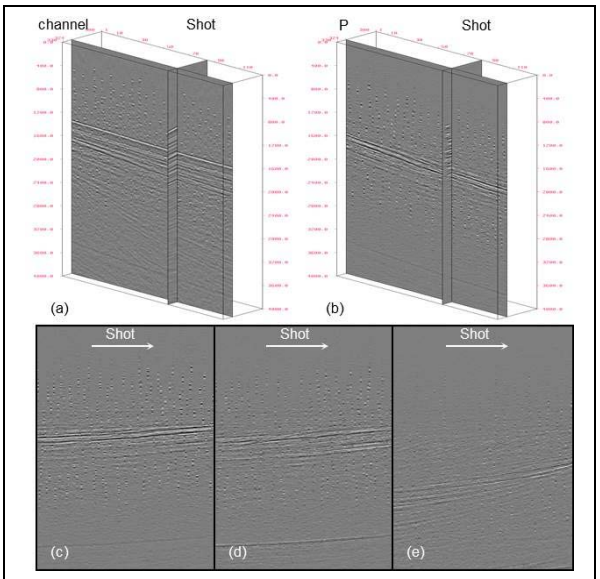

Figure 1: 2D sparse TauP transform along the channel direction; (a) input shot gathers window of 32 consecutive channels; (b) after shot domain 2D sparse TauP transform; (c), (d) and (e) are three common P gathers with different P values.

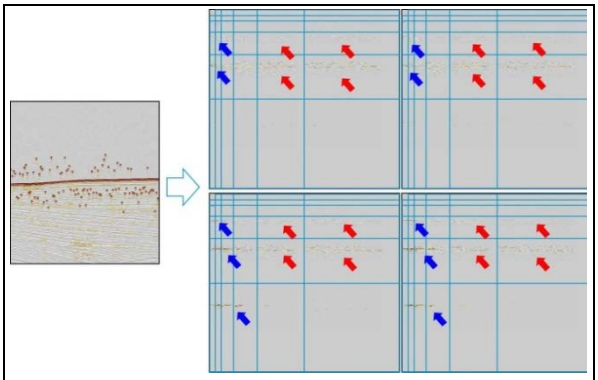

Figure 2: A 2D HARCWT example; *left:* the input blended gather; *right:* the complex transform coefficients; the left columns are real parts and the right columns are the imaginary parts; the upper row shows coefficients of bases with positive angles (direction from northwest to southeast), and the lower row shows the coefficients of bases with negative angles; the coefficients indicated by blue arrows represent the coherent events, and the weak coefficients indicated by red arrows represent the cross-talk energy.

Figure 2 shows an example of the transform for a blended gather. The coefficients representing coherent signals in the input are concentrated in the left panels where coefficients of bases with small dip angles reside (indicated by blue arrows). Due to the randomness, the coefficients of cross-talk are weak and distributed in large area, especially in top-right panels for bases with large dip angles (indicated by red arrows).

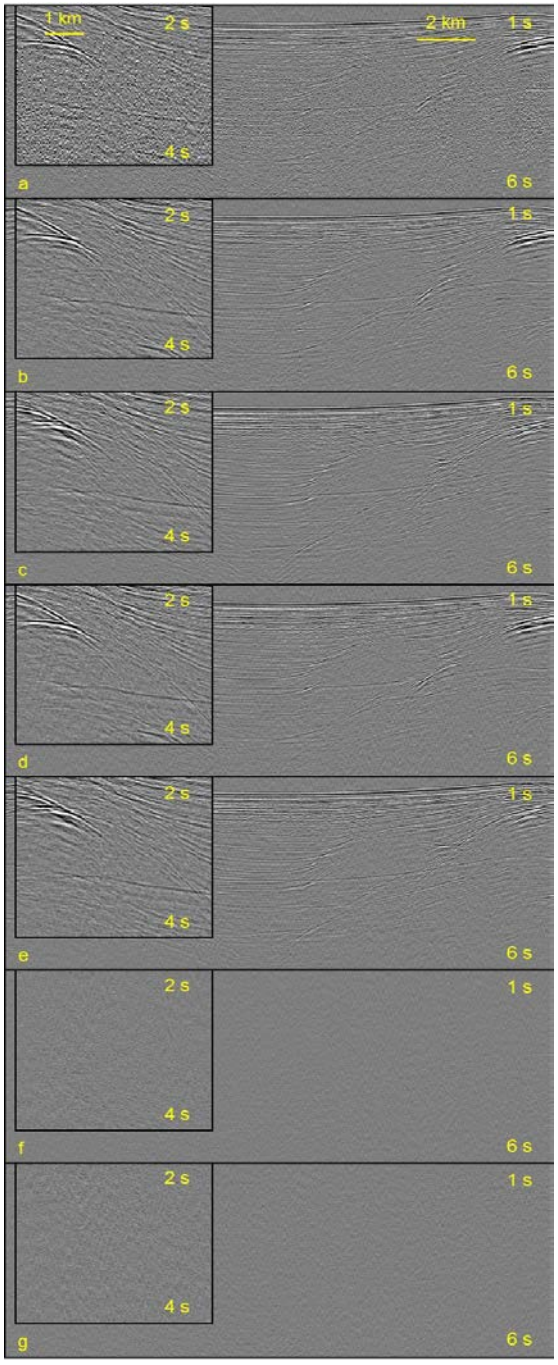

Figure 3: (a) blended common channel gather including a zoomed-in window; (b) source 1 before blending; (c) source 2 before blending; (d) deblended source 1 with the proposed method; (e) deblended source 2 with the proposed method; (f) the error between (b) and (d); (g) the error between (c) and (e).

For each P gather, we solve the following blending equation,

$$d = [\Gamma_1 \quad \dots \quad \Gamma_n]\begin{bmatrix} S & \cdots & 0 \\ \vdots & \ddots & \vdots \\ 0 & \cdots & S \end{bmatrix}\begin{bmatrix} H^T & \cdots & 0 \\ \vdots & \ddots & \vdots \\ 0 & \cdots & H^T \end{bmatrix}\begin{bmatrix} m_1 \\ \vdots \\ m_n \end{bmatrix} \quad (1),$$

where d is the blended common P gather; m_i is the model of source i in the 2D HARCWT domain; H^T is the backward 2D HARCWT operator; S is an interpolating operator to handle irregular grids and aliasing; and Γ_i is the shifting operator of source i. Equation (1) is an underdetermined linear system, hence no unique solution exists. We find a solution with the sparsest model in the HARCWT domain, which is equivalent to a constrained optimization problem as

$$\min\|\boldsymbol{m}\|_1 + \frac{\mu}{2}\|\boldsymbol{Ax} - \boldsymbol{d}\|_2^2 \ s.t.\ \boldsymbol{m} = \boldsymbol{Cx} \quad (2)$$

$$\boldsymbol{m} = [m_1, \dots, m_n]^{\mathrm{T}}, \boldsymbol{A} = [\Gamma_1 \quad \dots \quad \Gamma_n]\begin{bmatrix} S & \cdots & 0 \\ \vdots & \ddots & \vdots \\ 0 & \cdots & S \end{bmatrix}$$

$$\boldsymbol{C} = \begin{bmatrix} H & \cdots & 0 \\ \vdots & \ddots & \vdots \\ 0 & \cdots & H \end{bmatrix},$$

where x represents deblended common P gathers, and μ is the weight of the fitting errors, which can be used to adjust the sparsity of the HARCWT models for the deblended gathers. The alternating direction method of multipliers (ADMM) algorithm (Li, 2012) can be used to solve the problem.

Although the inversion is performed in 2D, our method honors 3D coherence of seismic events because the sparse TauP transform has focused coherent events along channels to certain P traces. Furthermore, the fine separation of events into different P traces by the sparse TauP transform can reduce the overlap of coherent signals with the cross-talk energy, since the overlapped events of different sources may have different slopes along the channel direction, e.g., when there is delay among different sources. This improves the deblending results.

Example

We tested our method on a numerically blended field data set. The field data came from the same survey, and the two sources were separated spatially by 1200 m along the crossline direction. The blending scheme involved a bulk shift of 2 seconds, plus random dithering from -1 second to +1 second. The shot interval was 25 m for the same source. We introduced the bulk shift for source 2 in order to allow the strong energy from source 2 to interact with the relatively weak energy from source 1, creating a challenging scenario for recovering the weak signal from source 1.

Figure 3(a) shows one common channel gather from the synthetically blended input; Figures 3(b) and (c) are the two unblended single source common channel gathers used to create the blending input, i.e., the ideal result for the deblending problem. We can observe some weak events in the deep parts of the unblended gathers. In the blended inputs, some weak events were masked by the cross-talk energy from the other source. Figures 3(d) and (e) show source 1 and source 2, respectively, deblended with our method. We observed that the weak diffraction signals of source 2 and the weak deep events of source 1 were recovered accurately. By taking the difference between the ideal data and the deblended results, the deblending errors were calculated and shown in Figure 3(f) and (g). The errors were small, and no obvious primary damage can be observed.

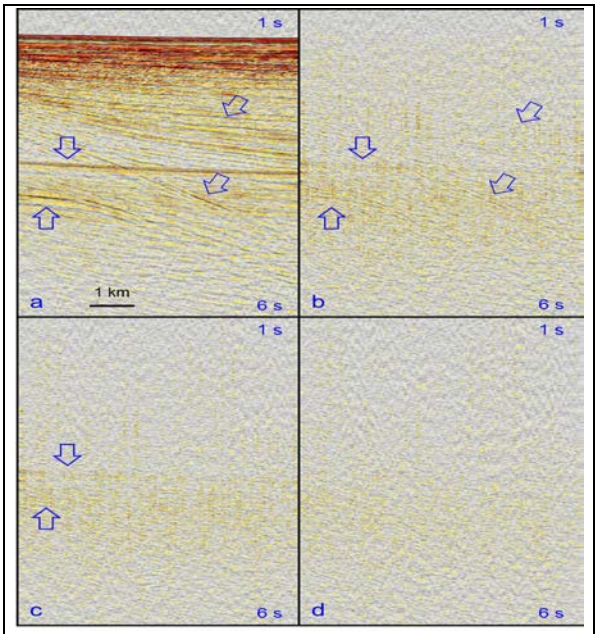

Figure 4: (a) Ideal single source image; (b) deblending error of 2D HARCWT inversion (+ 3dB gain); (c) deblending error of 3D HARCWT inversion (+ 3dB gain); (d) deblending error of the proposed method (+ 3dB gain).

Figure 4 compares the source 1 deblending errors of three methods: Figure 4(b), the 2D method based on 2D HARCWT and ADMM inversion for each common channel separately; Figure 4(c), the 3D method based on pure 3D HARCWT and ADMM inversion; and Figure 4(d), our 3D method. The error between the result of 2D inversion and the true answer contained relatively strong damage of coherent events at many locations, indicated by blue arrows in Figure 4(b). We noted that this damage was only visible in the difference between the true answer and the deblending result, and not in the inversion residual, i.e., the difference between the input and the re-blending of the deblending results. This implies that mistaken separation of the energy among sources may have happened in the 2D inversion deblending. This may be because the coherence of events in the channel direction was not taken into account during inversion, and strong cross-talk from source 2 made the recovery of the relatively weak events more difficult. The deblending error from the pure 3D HARCWT inversion (Figure 4(c)) was much smaller than that of the 2D inversion. 3D HARCWT honored the coherent signal in the channel direction; however, compared with the TauP transform, its dipping resolution was still not sufficient for high frequency signals. Therefore, some high frequency signal damage was observed. The deblending error of the proposed method was the smallest among these three, and no obvious signal damage was observed. Meanwhile, the proposed method was less expensive than 3D HARCWT inversion in terms of both CPU time and required memory.

Conclusions

We proposed a new method of 3D deblending for towed-streamer simultaneous source data by sequentially applying a 2D sparse TauP transform for each shot gather and performing 2D inversion-based deblending with HARCWT for common P gathers. This method considers the coherence of seismic events in both shot and channel directions, and was shown to outperform 2D deblending. Additionally, because this method decouples the sparse TauP transform from the inversion procedure, it does not heavily increase the computational cost; in certain situations it may even reduce the computational cost. We tested the method on a numerically blended field data set, for which the ideal deblending result was known. Comparisons of the deblending result of this method with the ideal result showed that both strong and weak seismic events were recovered well with only weak random energy in the difference.

As with other deblending algorithms, this method degrades in performance when the number of sources increases and the shot interval increases. Increasing the number of sources reduces the ratio of coherent energy to cross-talk, making coherent signal extraction with the sparse inversion less effective. Similarly, an increase in the shot interval reduces coherence in common channel gathers and makes signal extraction more difficult. Usually, reduction in firing time randomness severely degrades the deblending results of 2D methods; however, since our method first separates events with different slopes to different common P gathers, it is less sensitive to small dither time ranges.

Acknowledgements

We thank CGG for the permission to publish this work.

EDITED REFERENCES

Note: This reference list is a copyedited version of the reference list submitted by the author. Reference lists for the 2016 SEG Technical Program Expanded Abstracts have been copyedited so that references provided with the online metadata for each paper will achieve a high degree of linking to cited sources that appear on the Web.

REFERENCES

Abma, R. L., T. Manning, M. Tanis, J. Yu, and M. Foster, 2010, High quality separation of simultaneous sources by sparse inversion: 72nd Annual International Conference and Exhibition, EAGE, Extended Abstracts, B003, http://dx.doi.org/10.3997/2214-4609.201400611.

Akerberg, P., G. Hampson, J. Rickett, H. Martin, and J. Cole, 2008, Simultaneous source separation by sparse Radon transform: 78th Annual International Meeting, SEG, Expanded Abstracts, 2801–2805, http://dx.doi.org/10.1190/1.3063927.

Ayeni, G., and A. Almonmin, 2011, On the separation of simultaneous-source data by inversion: 81st Annual International Meeting, SEG, Expanded Abstracts, 20–25, http://dx.doi.org/10.1190/1.3627624.

Beasley, C., A. Salama, and W. H. Dragoset, 2011, A 3D simultaneous source field test processed by active separation: 73rd Annual International Conference and Exhibition, EAGE, Extended Abstracts, H030.

Beasley, C., I. Moore, D. Monk, and L. Hansen, 2012, Simultaneous sources: The inaugural full-field, marine seismic case history: 82nd Annual International Meeting, SEG, Expanded Abstracts, 1–5, http://dx.doi.org/10.1190/segam2012-0834.1.

Doulgeris, P., A. Mahdad, and G. Blacquiere, 2010, Separation of blended impulsive sources using an iterative approach: 72nd Annual International Conference and Exhibition, EAGE, Extended Abstracts, B004.

Kumar, R., H. Wason, and F. J. Herrmann, 2015, Source separation for simultaneous towed-streamer marine acquisition — A compressed sensing approach: Geophysics, **80**, no. 6, WD73–WD88, http://dx.doi.org/10.1190/geo2015-0108.1.

Li, C., C. C. Mosher, L. C. Morley, Y. Ji, and J. D. Brewer, 2013, Joint source deblending and reconstruction for seismic data: 83rd Annual International Meeting, SEG, Expanded Abstracts, 82–87, http://dx.doi.org/10.1190/segam2013-0411.1.

Li, C., S. T. Kaplan, and C. C. Mosher, 2012, An efficient variable-splitting multiplier method for compressive sensing seismic data reconstruction: 82nd Annual International Meeting, SEG, Expanded Abstracts, 1–6, http://dx.doi.org/10.1190/segam2012-1288.1.

Maraschini, M., R. Dyer, K. Stevens, and D. Bird, 2012, Source separation by iterative rank reduction — Theory and applications: 74th Annual International Conference and Exhibition, EAGE, Extended Abstracts, A044.

Peng, C., B. Liu, A. Khalil, and G. Poole, 2013, Deblending of simulated simultaneous sources using an iterative approach: An experiment with variable-depth streamer data: 83rd Annual International Meeting, SEG, Expanded Abstracts, 4278–4282, http://dx.doi.org/10.1190/segam2013-0214.1.

Peng, C., R. Huang, and B. Asmeron, 2013, Shear noise attenuation and PZ matching for OBN data with new scheme of complex wavelet transform: 83rd Annual International Meeting, SEG, Expanded Abstracts, 4251–4255, http://dx.doi.org/10.1190/segam2013-0634.1.

Trad, D., T. Ulrych, and M. Sacchi, 2003, Latest views of the sparse Radon transform: Geophysics, **68**, 386–399, http://dx.doi.org/10.1190/1.1543224.